Exotic Harmonic Generation Schemes in High-Gain, Free-Electron Lasers

Sandra G. Biedron[1,2], Riccardo Bartolini[3], Franco Ciocci[3], Giuseppe Dattoli[3], William M. Fawley[4], Giuseppe Felici[3], Henry P. Freund[5], Heinz-Dieter Nuhn[6], Pier Luigi Ottaviani[7], Alberto Renieri[3]

[1]Advanced Photon Source, Argonne National Laboratory, Argonne, IL 60439 USA
[2]Also at MAX-Laboratory, University of Lund, Lund, Sweden SE-221 00
[3]ENEA, Divisione Fisica Applicata, Centro Ricerche Frascati, C.P. 65, 00044 Frascati, Rome, Italy
[4]Lawrence Berkeley National Laboratory, Berkeley, CA 94720, USA
[5]Science Applications International Corp., McLean, VA 22102 USA
[6]Stanford Linear Accelerator Center, Stanford, CA 94309 USA
[7]ENEA, Divisione Fisica Applicata, Centro Ricerche E. Clementel, Via Don Fiammelli, Bologna, Italy

SPIE paper # 4632-35

LASE 2002
High-Power Lasers and Applications
Directed Energy
Laser and Beam Control Technologies

part of SPIE's Photonics West
22-24 January 2002
San Jose, CA

Exotic Harmonic Generation Schemes in High-Gain, Free-Electron Lasers

Sandra G. Biedron[1,2], Riccardo Bartolini[3], Franco Ciocci[3], Giuseppe Dattoli[3], William M. Fawley[4], Giuseppe Felici[3], Henry P. Freund[5], Heinz-Dieter Nuhn[6], Pier Luigi Ottaviani[7], Alberto Renieri[3]

[1]Advanced Photon Source, Argonne National Laboratory, Argonne, IL 60439 USA
[2]Also at MAX-Laboratory, University of Lund, Lund, Sweden SE-221 00
[3]ENEA, Divisione Fisica Applicata, Centro Ricerche Frascati, C.P. 65, 00044 Frascati, Rome, Italy
[4]Lawrence Berkeley National Laboratory, Berkeley, CA 94720, USA
[5]Science Applications International Corp., McLean, VA 22102 USA
[6]Stanford Linear Accelerator Center, Stanford, CA 94309 USA
[7]ENEA, Divisione Fisica Applicata, Centro Ricerche E. Clementel, Via Don Fiammelli, Bologna, Italy

ABSTRACT

The mechanism of nonlinear harmonic generation in the exponential gain regime, which is driven by bunching at the fundamental wavelength, may provide a path toward both enhancing and extending the usefulness of an x-ray free-electron laser (FEL) facility. Related "exotic" generation schemes, which exploit properties of harmonic production in various undulator topologies, have been discussed both in the past and more recently. Using three different numerical simulation codes, we explore the possible utility of such schemes (e.g., harmonic "afterburners" and biharmonic undulators) at future light source facilities.

Keywords: Free-electron laser, FEL, self-amplified spontaneous emission, SASE, nonlinear harmonics, after-burners, SASE, harmonic generation, frequency conversion, two-undulator harmonic generation scheme, TUHGS, intense particle beams, and radiation sources

1. INTRODUCTION

Some of the desired characteristics of a next-generation light source [1,2,3,4] user facility include

- tunable to ultrashort wavelengths including the 1-10 keV x-ray regime,
- longitudinal coherence,
- transverse coherence,
- ultrashort pulse durations (<100 fs),
- high peak powers, and
- as small and as cost-effective as reasonably possible.

A possible method of achieving this wish list is with a high-gain, single-pass, free-electron laser (FEL). Some uses for such devices include flash imaging of biomolecules and X-ray holography and high-resolution imaging that rely on the property of coherence; dynamics of atomic, molecular, and biological systems that rely on the 100-fs to 10-ps time domain; and, nonlinear physics that relies upon the ultrahigh peak power.

There are a number of single-pass, high-gain FEL configurations that can operate in the short wavelength (suboptical) range. In an FEL amplifier, an electron beam traversing a periodic undulator can amplify radiation from a seed laser if the standard FEL resonance condition is obeyed. The seed laser induces an energy modulation onto the electron beam, giving a memory of the longitudinal and transverse coherence properties on the electron beam. The FEL interaction continues to amplify the radiation field until the resultant increased energy spread on the electron beam "saturates" the gain. An alternative approach is that of self-amplified spontaneous emission (SASE) [5], which starts up from the random microbunching (i.e., shot noise) on the

electron beam instead of being coherently produced by an input seed laser source. This source is fully transversely coherent at saturation, but, due to the fact that the radiation starts up from random noise at many radiation wavelengths, the longitudinal coherence of the radiation is less than that of the amplifier case but better than that of spontaneous radiation. Next, there are two methods for frequency up-conversion of a radiation pulse: the two-undulator harmonic generation scheme (TUHGS), otherwise known as an "afterburner" [6,7,8], and the high-gain harmonic generation (HGHG) scheme [9,10,11]. Both approaches, via a seed laser and FEL amplification in a first undulator, produce strong microbunching of the electron beam. The microbunched beam is then injected into a second undulator that is tuned in resonance (for the same electron beam energy) to a higher harmonic wavelength of the initial seed laser. This second device then acts as a coherent radiator. In both configurations, the second undulator produces radiation power approaching that of a system tuned only to the shorter harmonic wavelength with an electron beam operated at a higher energy necessary for resonance.

In all of the above-listed methods, there exists nonlinear harmonic generation resulting from the strong electron beam microbunching present at the fundamental wavelength [12,13,14,15,16,17]. These harmonics experience gain similar to that of the fundamental with gain lengths scaling as the inverse of the harmonic number. Nonlinear harmonic generation in FELs is a promising method to reach shorter wavelengths with more ease than the current designs allow, since it does not require as high an electron beam energy for the same desired output. For linearly polarized magnetic undulators, the odd harmonics are favored as they couple more closely to the natural undulative motion of the electron beam through the device. Finally, nonlinear harmonic radiation can itself be an output source or, alternatively, could serve as a seed for further FEL amplification at shorter wavelengths [18].

Since the nonlinear harmonics result from the microbunching at the fundamental wavelength, we have suggested that their sensitivity to electron beam quality (energy spread, emittance, and peak current) and/or undulator errors would be comparable to that of the FEL interaction at the fundamental. In our group's recent work, we investigated the effects of emittance, energy spread, and peak current on the fundamental nonlinear harmonic generation in single-pass, high-gain, free-electron lasers with parameters similar to the first experiment of the low-energy undulator test line (LEUTL) at the Advanced Photon Source (APS) at Argonne National Laboratory (ANL) [19,20] as well as at the Linac Coherent Light Source (LCLS) [21]. We have also investigated the effect of wiggler errors on the fundamental and nonlinear harmonics for this same LCLS-like case and found the nonlinear harmonic output power followed that of the fundamental [22]. For both the long and short wavelength case studies, we found that the sensitivity of the nonlinear harmonic bunching and output power clearly followed that of the fundamental and was not extraordinarily great.

Parallel to these theoretical investigations, there have been measurements of 1) the nonlinear harmonic content in the joint Argonne National Laboratory (ANL) and Brookhaven National Laboratory (BNL) High-Gain Harmonic Generation (HGHG) experiment at the Accelerator Test Facility (ATF) at BNL [16,17,23] and 2) the power of fundamental and second harmonic radiation, microbunching magnitude, and spectrum as a function of distance at the LEUTL APS SASE FEL [20,24,25,26,27]. Harmonic spectral measurements at the Institute of Scientific and Industrial Research in Osaka University, Japan [28,29] and nonlinear harmonic spectral, intensity, and CTR measurements at the VISA (Visible to Infrared SASE FEL) experiment at BNL [30] have also been made.

In this paper, we turn to numerical investigation of the efficacy of biharmonic undulators and TUHGS schemes in producing short-wavelength radiation in FELs. Again, our primary interest is too see if lower energy electron beams can be utilized in nonstandard undulator configurations to reach shorter wavelengths at interesting power levels that normally are possible (in standard configurations) with much higher energy electron beams.

2. THEORETICAL INVESTIGATION TOOLS

At present, our group uses its three numerical simulation codes to investigate exotic free-electron laser schemes. These tools are briefly described here.

2.1 GINGER

GINGER is a multidimensional (3D macroparticle motion, 2D (r-z) radiation field), polychromatic FEL simulation code [31]. The equations of motion are averaged over an undulator period following the standard KMR [32] formulation while an eikonal approximation in time and space is used for the field propagation. For polychromatic SASE simulations, GINGER can be initiated with either electron beam shot noise or, alternatively, photon noise. In monochromatic mode the radiation is presumed to be at a single discrete wavelength. Macroparticle bunching in the longitudinal plane can be diagnosed through approximately the 9th harmonic (with the accuracy dependent upon macroparticle statistics); however, GINGER presently calculates and propagates radiation only within a narrow bandpass centered upon the fundamental wavelength. Thus, the effects of any emitted harmonic radiation upon the electron beam are ignored, which, in general, is a very good approximation up to saturation.

2.2 MEDUSA

MEDUSA is a 3D, multifrequency, macroparticle simulation code that represents the electromagnetic field as a superposition of Gauss-Hermite modes and uses a source-dependent expansion to determine the evolution of the optical mode radius [33,34,35,14]. The field equations are integrated simultaneously with the Lorentz force equations. MEDUSA differs from other nonlinear simulation codes in that no undulator-period averaging is imposed on the electron dynamics. It is capable of treating quadrupole and corrector fields, magnet errors, and multiple segment undulators of various quantities and types. MEDUSA is able to treat the fundamental and all harmonics simultaneously as well as treat sideband growth.

2.3 PROMETEO

PROMETEO is a 1D, multiparticle code [36] based on a modified version of the Prosnitz, Szoke, and Neil formulation of the FEL dynamical equations [37,38]. The original model has been generalized to include the effect of beam emittance and the undulator errors. The code is capable of accounting for the evolution of the fundamental harmonics and for the coherent generation of higher-order harmonics in SASE or oscillator FELs, including optical klystron and segmented undulators.

2.4 Recent Enhancements

Recently, PROMETEO and MEDUSA have been enhanced by adding the capability of simulating biharmonic undulators. The undulator actually consists of two sets of pole pieces situated at ninety degrees to one another. We have therefore termed these devices perpendicular biharmonic undulators. The wavelength of one pole set is tuned to a harmonic of the other.

3. SENSITIVITY OF NONLINEAR HARMONIC GENERATION IN AN FEL

Previously, we compared the codes GINGER, MEDUSA, and PROMETEO to one another at the fundamental and the higher harmonics in the case of the first operational phase of the low-energy undulator test line (LEUTL) FEL at the APS. These parameters are listed in Table 1. The LEUTL FEL is a successful prototype next-generation light source that is operational in its present configuration between the infrared and the vacuum ultraviolet wavelengths [39]. The first user experiments will be installed at the end of 2002.

For the first operational phase of the LEUTL FEL, we simulated a single, long segment of undulator with curved pole-face focusing. For each of the three codes, we executed a number of runs to scan either the radiation wavelength (for MEDUSA and PROMETEO) or undulator strength parameter K (for GINGER) while holding all other parameters fixed to find the minimum exponential gain length. We ran our three codes

in the amplifier case, each introducing an input fundamental seed power of 10 W to our three model systems, respectively. In other words, we did not start up the systems from noise on the fundamental. Also, we started the harmonics powers at zero power, in order to demonstrate the harmonic growth as a result of the electron beam microbunching at the fundamental wavelength. In addition, in each case we adopted a Gaussian electron beam profile in the transverse phase space. After performing these initial comparisons at the fundamental wavelength, we began the investigations of the variation of normalized emittance, energy spread, and peak current on the fundamental and nonlinear harmonics. Recall that GINGER is able to provide the fundamental power and bunching as well as bunching of the nonlinear harmonics, and MEDUSA and PROMETEO are able to simulate the fundamental and nonlinear harmonic powers and bunching. For comparison purposes, to lowest order, the power scales as the square of the bunching.

A harmonic sensitivity study to electron beam emittance, energy spread, and peak current was performed. The normalized electron beam emittance, energy spread, and peak current were varied between 1.0 and 10.0 π mm mrad, 0.0 and 2.0%, and 75 and 200 A, respectively, to calculate the effects on the fundamental and nonlinear harmonic bunching and power [20]. We also performed a SASE run, one that starts up from noise, for the nominal case to demonstrate the comparison to the amplifier cases. No significant differences appeared. We concluded that the nonlinear harmonics are only mildly more sensitive to the electron beam quality than the fundamental.

Parameter	*Value*
Electron beam γ	430.53
Electron beam energy (MeV)	219.5
Normalized electron beam emittance (π mm mrad)	5
Electron beam peak current (A)	150
Electron beam energy spread (%)	0.1
Undulator period, λ_{und} (cm)	3.3
Undulator strength parameter K	3.1
Fundamental radiation wavelength, λ_{rad} (nm)	517

Table 1: Parameters of the LEUTL FEL case.

We have also performed comparisons of these codes to one another at the fundamental and higher harmonics in a shorter wavelength regime. The case we examined was that of the LCLS-like case as shown in Table 2. The LCLS will be a prototype next-generation light source at the Stanford Linear Accelerator Center (SLAC). It will utilize the last third (1 km) of the SLAC linear accelerator as well as the addition of a photocathode-rf gun, one or more electron bunch-compression systems, and a 100-m undulator tuned in resonance with the electron beam to yield 1.5 Å radiation.

Parameter	*Value*
Electron beam γ	28085
Electron beam energy (MeV)	14.35
Normalized electron beam emittance (π mm mrad)	1.5
Electron beam peak current (A)	3400
Electron beam energy spread (%)	0.006
Undulator period, λ_{und} (cm)	3.0
Undulator strength parameter K	3.7
Fundamental radiation wavelength, λ_{rad} (nm)	0.15

Table 2: Parameters of the LCLS-like case.

For this LCLS-like case, we again simulated a single, long segment of undulator with curved pole-face focusing. For each of the three codes, we again executed a number of runs to scan either the radiation wavelength (for MEDUSA and PROMETEO) or undulator strength parameter K (for GINGER) while holding all other parameters fixed to find the minimum exponential gain length. We again ran our three codes in the amplifier case, each introducing an input seed power of 480 W to our three model systems, respectively. In addition, in each case, we simulated a Gaussian electron beam profile in the transverse phase space.

Harmonic sensitivity studies to electron beam emittance, energy spread, and peak current were performed. The normalized electron beam emittance, energy spread, and peak current were varied between 1.0 and 5.0 π mm mrad, 0.0 and 0.025%, and 3000 and 4000 A, respectively, to calculate the effects on the fundamental and nonlinear harmonic bunching and power [21]. A previous investigation performed simulations of the same case study with induced undulator errors and no great difference between the fundamental and harmonics appeared [22]. We concluded that the nonlinear harmonics are only mildly more sensitive to the electron beam quality than the fundamental.

Another related sensitivity comparison was performed on the high-gain harmonic generation scheme. Scans of the input seed laser power, electron beam energy spread, electron beam peak current, electron beam emittance, and dispersive section strength were conducted. Overall, the effect of the nonlinear harmonic output powers tracked that of the fundamental's behavior for each examined parameter [40]. Currently, we are in the process of examining the sensitivity of the biharmonic undulator devices and the TUHGS/afterburner schemes. Based upon all of the above-summarized work, we do not expect any large deviation of the harmonic bunching or power from the trend of the fundamental bunching or power based upon the results of the previous work in either TUHGS or biharmonic undulator schemes.

4. CURRENT INVESTIGATIONS

We have performed simulations to compare the high-gain FEL output radiation output from biharmonic undulators, monoharmonic undulators, and an exotic scheme of an afterburner (TUHGS) with two monoharmonic undulators. Biharmonic undulators for FELs have been investigated previously. In a Compton free-electron laser in the oscillator regime, Ircane et al. saw a strong enhancement of the harmonic generation in simulation with the fundamental and harmonic magnetic components positioned in parallel planes [41]. Asakawa et al. examined the possible enhancement of the harmonic-to-fundamental ratio in the low-gain regime for a modified, parallel biharmonic wiggler using the 1D theory and also measured enhanced third-harmonic spontaneous emission [42]. Recently, we have performed detailed investigations using a biharmonic undulator in next-generation light sources [43,44]. To reduce the broadband spontaneous emission, we keep the well-known undulator strength parameter K the same for both "undulators." The new resonance condition is given by

$$\lambda_{rad} = \frac{\lambda_{und}}{2\gamma^2}\left(1+\frac{K_1^2}{2}+\frac{K_h^2}{2}\right) = \frac{\lambda_{und}}{2\gamma^2}\left(1+K_0^2\right),$$

where K_1 and K_h correspond, respectively, to the undulator strength parameter K for the fundamental and harmonic and, since we already mentioned that both undulator strength parameters should be of the same value, this same value is denoted as K_0, and the parameters can now be added together.

Using GINGER, we simulated an afterburner case (TUHGS). Using MEDUSA and PROMETEO, we simulated the purely nonlinear harmonic case, the biharmonic case with perpendicular harmonic pole faces, as well as the TUHGS/afterburner case. Table 3 lists the parameters of the three cases studies. In Figure 1 we see the power (W) versus distance for the TUHGS case where the first undulator ends and the second undulator starts at z = 51 m. The first undulator is cut at this point to keep the FEL-induced electron beam energy spread sufficiently low to maintain the efficiency of the afterburner. Figure 2 shows the fundamental and harmonic bunching versus distance through both sections of undulator. Note that GINGER is capable of calculating the fundamental and harmonic bunching as well as the fundamental power for a given undulator. The summary of the results of this case using GINGER is listed in Table 4.

Case	*A*	*B*	*C*
Undulator type	Monoharmonic	Biharmonic (perpendicular poles)	TUHGS
Electron beam energy (MeV)	935	1078	935
Normalized electron beam emittance (π mm mrad) [x,y]	1, 1	1, 1	1, 1
Electron beam peak current (A)	850	850	850
Energy spread (%)	0.05	0.05	0.05
Resonant wavelength of undulator(s)	At fundamental only	At fundamental and third harmonic	First at fundamental only and second at third harmonic only
Undulator period, λ_{und} (cm)	6.0	6.0	6.0
Third harmonic undulator period (cm)	-na-	2.0	2.0
Peak magnetic field (kG)	1.767	1.767	First 1.767
Peak magnetic field (kG) of third harmonic undulator	-na-	5.301	Second 5.301
Fundamental wavelength (nm)	13.36	13.36	13.36
Third harmonic wavelength (nm)	4.45	4.45	4.45
Ninth harmonic wavelength (nm)	1.48	1.48	1.48

Table 3: Parameters of the simulated monoharmonic, biharmonic, and TUHGS cases.

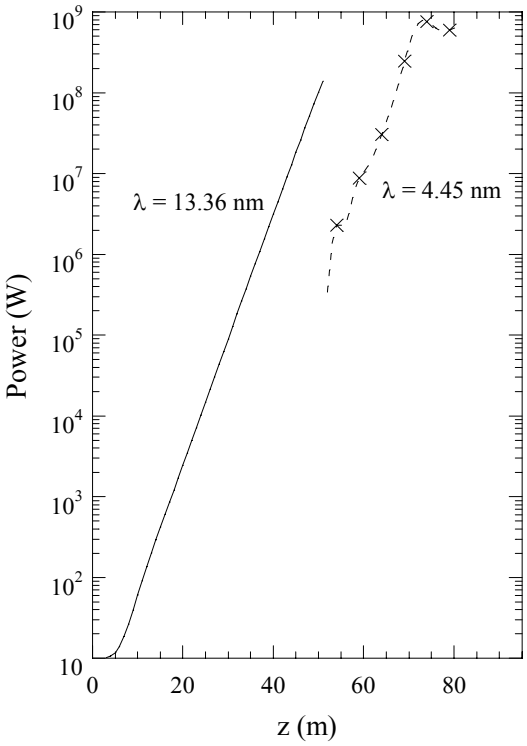

Figure 1: Power versus distance of the TUHGS simulation run using GINGER where the first undulator ends and the second undulator begins at z = 51 m.

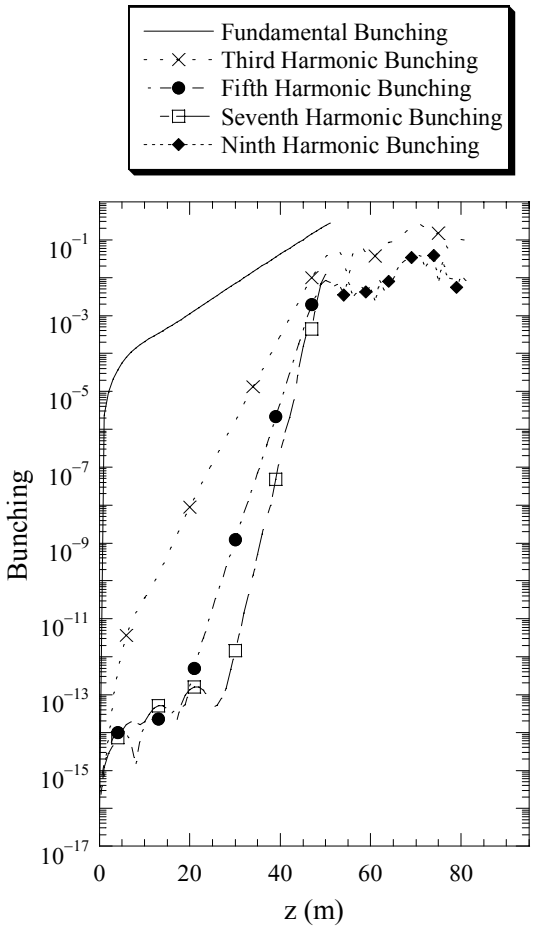

Figure 2: Bunching versus distance of the TUHGS simulation run using GINGER where the first undulator ends and the second undulator begins at z = 51 m.

Type	Fundamental (14.45 nm)	Third (4.45 nm)	"Saturation" z (m)	Energy (MeV)
TUHGS (Undulator 1 ends at 51 m)	139 MW (z = 51 m)	786.7 MW (z = 73 m)	73 m	935

Table 4: Summary of the simulated TUHGS case results using GINGER.

In Figures 3, 4, 5, and 6, we see power (W) versus distance (m) plots resulting from the simulations of the purely nonlinear harmonic case, the biharmonic case, as well as two TUHGS cases, respectively, produced using MEDUSA. The length of the first undulator was first made to be long enough that the fundamental reached saturation (as demonstrated in Figure 5). Then, the first undulator was ended before the FEL-induced energy spread was significant (as demonstrated in Figure 6). The summary of the results of these three cases using MEDUSA are listed in Table 5. Note that in this tabular summary we have measured the nonlinear harmonic power and bunching at the point at which the fundamental saturates.

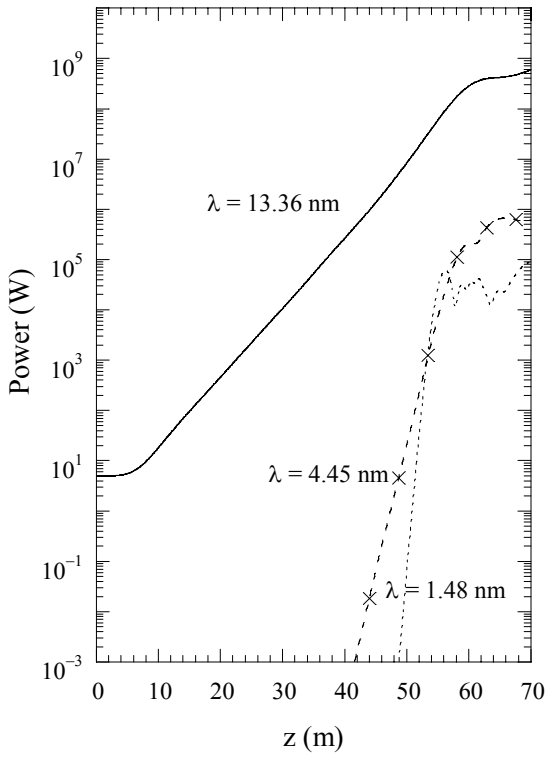

Figure 3: Power versus distance of the monoharmonic undulator simulation run using MEDUSA.

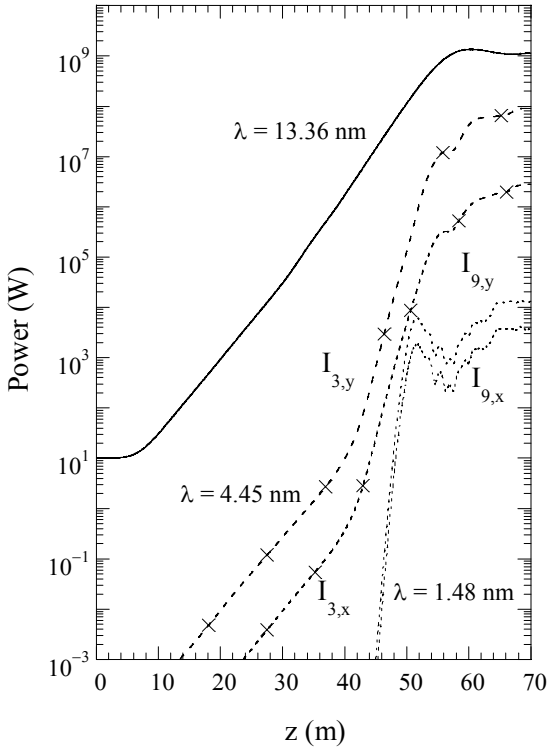

Figure 4: Power versus distance of the biharmonic undulator simulation run using MEDUSA.

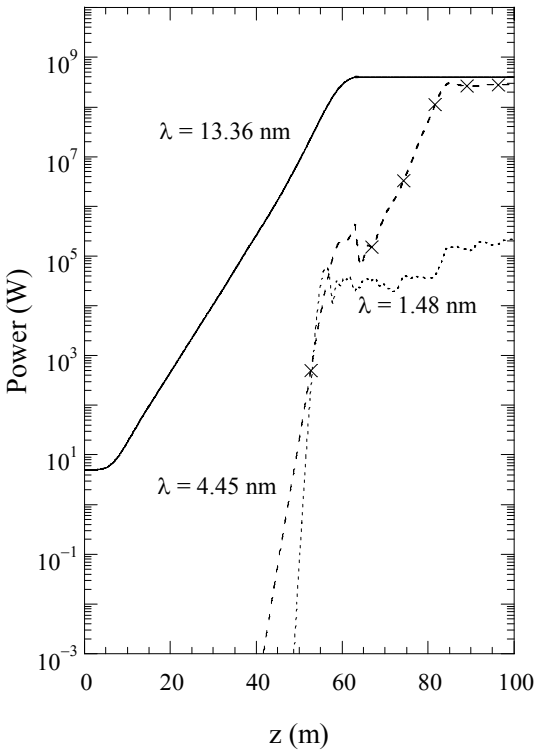

Figure 5: Power versus distance of the TUHGS simulation run using MEDUSA where the first undulator ends and the second undulator begins at z = 63 m.

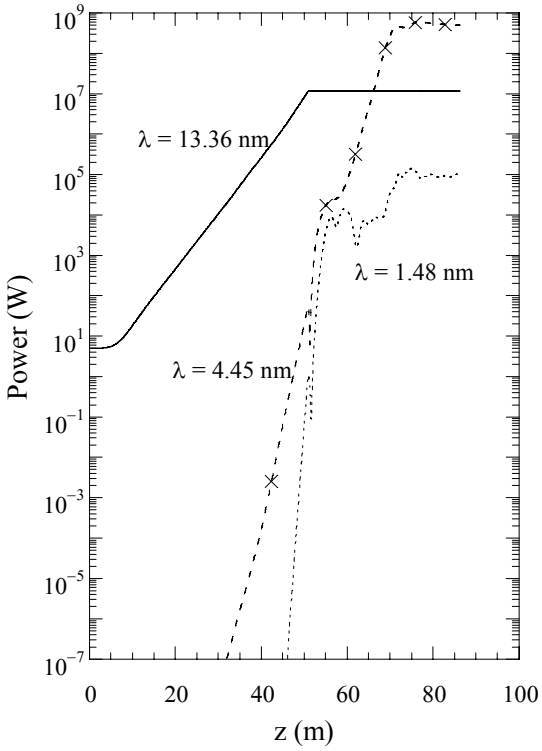

Figure 6: Power versus distance of the TUHGS simulation run using MEDUSA where the first undulator ends and the second undulator begins at z = 51 m.

Type	Fundamental (13.36 nm)	Third (4.45 nm)	Ninth (1.48 nm)	"Saturation" z (m)	Energy (MeV)
Monoharmonic	398 MW	0.64 MW	50 kW	~ 60	935
Biharmonic	1270 MW	52 MW in y-pol.	5 kW	~ 60	1078
TUHGS (Undulator 1 ends at 63 m)	398 MW (z = 63 m)	0.424 MW (z = 63 m) 300 MW (z = 84 m)	19.42 kW (z = 63 m) 0.373 MW (z = 84 m)	~ 80	935
TUHGS (Undulator 1 ends at 51 m)	11.8 MW (z = 51 m)	56.9 W (z = 51 m) 460 MW (z = 74 m)	1.02 W (z = 51 m) 0.15 MW (z = 74 m)	~74	935

Table 5: Summary of the simulated monoharmonic, biharmonic, and two TUHGS case results using MEDUSA.

In Figures 7, 8, 9, and 10 we see the power (W) versus distance (m) plots resulting from the simulations of the purely nonlinear harmonic case, the biharmonic case, as well as two TUHGS cases, respectively, produced PROMETEO. The length of the first undulator was first made to be long enough that the fundamental reached saturation (as demonstrated in Figure 9). Then, the first undulator was ended before the FEL-induced energy spread was significant (as demonstrated in Figure 10). The summary of the results of these cases using PROMETEO is listed in Table 6. Finally, in the case of TUHGS, PROMETEO predicts a different behavior with respect to MEDUSA when the undulator is cut at 63 m. The reduced power in the third harmonic is caused by the FEL-induced electron beam energy near saturation in the first section. Here, further reduction is presumably due to the one-dimensional nature of PROMETEO, which is unable to simulate the three-dimensional effects.

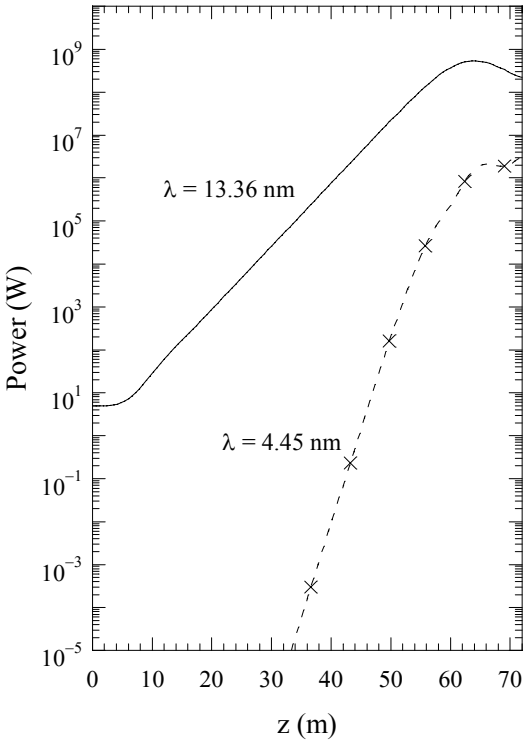

Figure 7: Power versus distance of the monoharmonic undulator simulation run using PROMETEO.

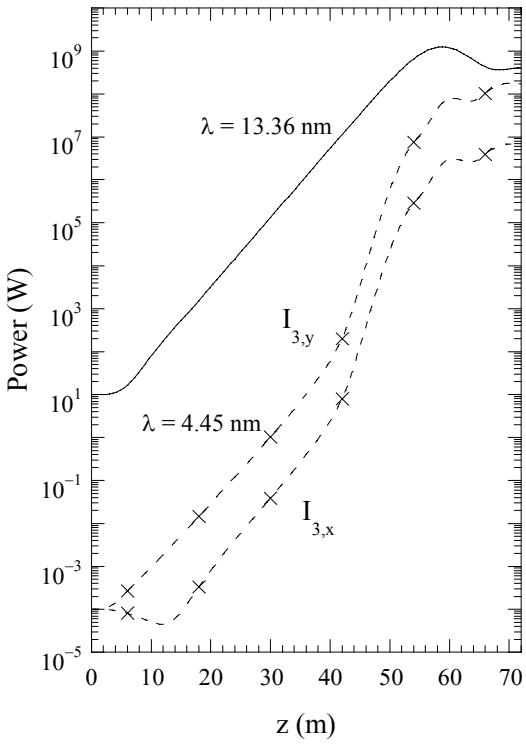

Figure 8: Power versus distance of the biharmonic undulator simulation run using PROMETEO.

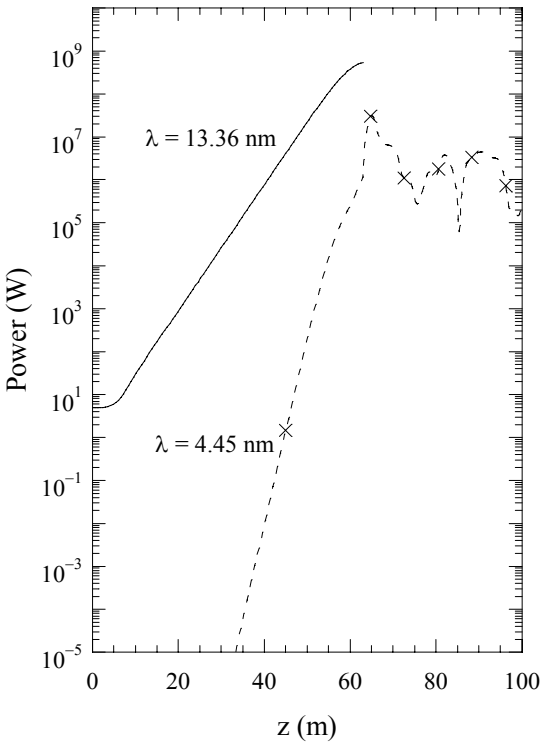

Figure 9: Power versus distance of the TUHGS simulation run using PROMETEO where the first undulator ends and the second undulator begins at z = 63 m.

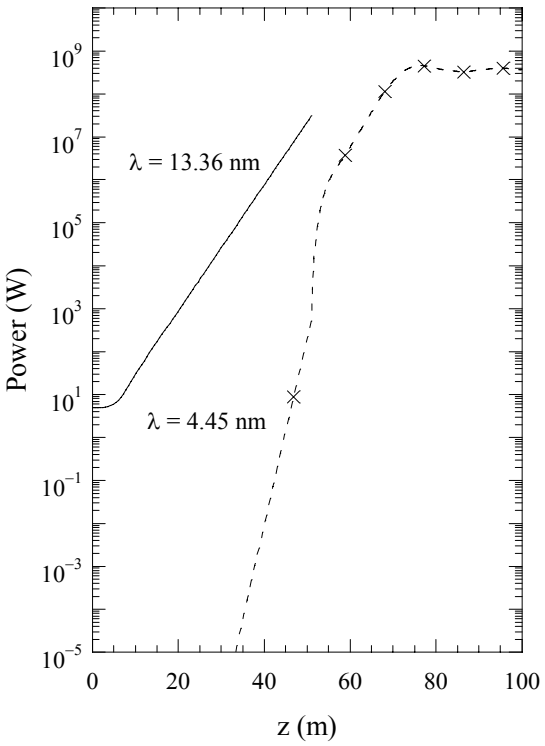

Figure 10: Power versus distance of the TUHGS simulation run using PROMETEO where the first undulator ends and the second undulator begins at z = 51 m.

Type	Fundamental (13.36 nm)	Third (4.45 nm)	"Saturation" z (m)	Energy (MeV)
Monoharmonic	533 MW	1.69 MW	64	935
Biharmonic	1239 MW	61 MW in y-pol	59	1078
TUHGS (Undulator 1 ends at 63 m)	530 MW (z = 63)	1.16 MW (z = 63) 31 MW (z = 65)	65	935
TUHGS (Undulator 1 ends at 51 m)	30.6 MW (z = 51)	519 W (z = 51) 453 MW (z = 76)	76	935

Table 6: Summary of the simulated monoharmonic, biharmonic, and TUHGS case results using PROMETEO.

5. SUMMARY AND CONCLUSIONS

Nonlinear harmonic generation is an important attribute of high-gain FELs. In this paper we have studied and compared several harmonic generation configurations including two-undulator harmonic generation schemes (TUHGS), biharmonic undulators, and the nonlinear harmonics in these systems as well as in monoharmonic undulators. These schemes produce enhanced harmonic emission with powers within an order of magnitude of one another, particularly in the cases of the TUHGS and biharmonic undulators. Each scheme offers various advantages for a specific user's requirements. Biharmonic undulators and TUHGS schemes may be important in driving the desired harmonic to a higher level within a given undulator length.

ACKNOWLEDGEMENTS

The authors wish to thank their frequent collaborators — Drs. Zhirong Huang, Kwang-Je Kim, John W. Lewellen, and Stephen Val Milton — for their support and many discussions regarding this manuscript.

The work of S.G. Biedron is supported at Argonne National Laboratory by the U.S. Department of Energy, Office of Basic Energy Sciences under Contract No. W-31-109-ENG-38. The activity and computational work of H. P. Freund is supported by Science Applications International Corporation's Advanced Technology Group under IR&D subproject 01-0060-73-0890-000. The activity of W.M. Fawley is supported at Lawrence Berkeley National Laboratory by the U.S. Department of Energy under Contract No. DE-AC03-76SF00098. The work of H.-D. Nuhn is supported by the U.S. Department of Energy, Office of Basic Energy Sciences, Division of Material Sciences, under Contract No. DE-AC03-76SF00515. The work of R. Bartolini, F. Ciocci, G. Dattoli, G. Felici, P.L. Ottaviani, and A. Renieri is supported by ENEA the Italian Agency for New Technologies, Energy, and the Environment.

REFERENCES

1. LCLS Design Study Report, SLAC-R-521, Rev. 1998, UC-414.
2. LCLS: The First Experiments, September 2000, SLAC report for the U.S. Department of Energy, BESAC Committee (Basic Energy and Sciences Committee) held 10-11 October 2000 in Washington, D.C.
3. TESLA: The Superconducting Electron-Positron Linear Collider with an Integrated X-Ray Laser Laboratory, Technical Design Report, TESLA Report 2001-23 (2001).
4. Proceedings of the Workshop on the Generation and Uses of VUV and Soft X-Ray Coherent Pulses, July 17-20, 2001, Lund, Sweden, C. Eyberger, S.G. Biedron, S.V. Milton, and K. Jaje, editors, in press.
5. A.M. Kondratenko and E.L. Saldin, Sov. Phys. Dokl. 24 (12) (1979) 986.
6. R. Bonifacio et al., Nucl. Instum. Meth. A 296 (1990) 787.
7. F. Ciocci et al., IEEE J. Quant. Electron. 31 (1995) 1242.
8. W.M. Fawley et al., Proceedings of the IEEE 1995 Particle Accelerator Conference (1996) 219.
9. L.-H. Yu, Phys. Rev. A 44 (1991) 5178.
10. I. Ben-Zvi et al., Nucl. Instrum. Meth. A 318 (1992) 208.
11. L.-H. Yu et al., Science 289 (2000) 1932.
12. R. Bonifacio et al., Nucl. Instr. Meth. A 293 (1990) 627.
13. G. Dattoli and P.L. Ottaviani, J. Appl. Phys. 86 (1991) 5331.
14. H.P. Freund, S.G. Biedron, and S.V. Milton, IEEE J. Quant. Electron. 36 (2000) 275.
15. Z. Huang and K.-J. Kim, Phys. Rev. E 62 (2000) 7295.
16. S.G. Biedron et al., Nucl. Instrum. Meth. A 475 (2001) 118.
17. A. Doyuran et al., Nucl. Instrum. Meth. A 475 (2001) 260-265.
18. S.G. Biedron, H.P. Freund, and S.V. Milton, Nucl. Instrum. Meth. A 475 (2001) 401.
19. S.G. Biedron, G. Dattoli, H.P. Freund, Z. Huang, S.V. Milton, H.-D. Nuhn, P.L. Ottaviani, and A. Renieri, "High-Gain Free-Electron Lasers and Harmonic Generation," Physics of, and Science with, the X-Ray Free-Electron Laser, 19th Advanced ICFA Beam Dynamics Workshop; Edited by M. Cornacchia, Stanford Linear Accelerator Center, Stanford, CA, USA; C. Pellegrini, Department of Physics and Astronomy, University of California at Los Angeles, Los Angeles, CA, USA; S. Chattopadhyay, Jefferson

Lab, Newport News, VA, USA; I. Lindau, Stanford Linear Accelerator Center, Stanford, CA, USA August 2001, 0-7354-0022-9, CP 581 (2001) 203.
20. S.G. Biedron, G. Dattoli, W.M. Fawley, H.P. Freund, Z. Huang, K.-J. Kim, S.V. Milton, H.-D. Nuhn, P.L. Ottaviani, and A. Renieri, "Impact of Electron Beam Quality on Nonlinear Harmonic Generation in High-Gain Free-Electron Lasers," Proceedings of the 21st ICFA Beam Dynamics Workshop on LASER-BEAM INTERACTIONS, Stony Brook, USA, June 11-15, 2001 and Phys. Rev. Special Topics, Accelerators and Beams, Special Conference Edition, Volume 5, 030701 (2002).
21. S.G. Biedron, G. Dattoli, W.M. Fawley, H.P. Freund, Z. Huang, K.-J. Kim, S.V. Milton, H.-D. Nuhn, P.L. Ottaviani, and A. Renieri, "The Sensitivity of Nonlinear Harmonic Generation to Electron Beam Quality in Free-Electron Lasers," Nucl. Instrum. Meth. A, accepted and in press.
22. H.P. Freund, S.G. Biedron, S.V. Milton, and H.-D. Nuhn, IEEE J. of Quantum Electronics, 37 (2001) 790.
23. A. Doyuran, M. Babzien, T. Shaftan, L.H. Yu, L.F. DiMauro, I. Ben-Zvi, S.G. Biedron, W. Graves, E. Johnson, S. Krinsky, R. Malone, I. Pogorelsky, J. Skaritka, G. Rakowsky, X.J. Wang, M. Woodle, V. Yakimenko, J. Jagger, V. Sajaev, and I. Vasserman, PRL 86 (2001) 5902.
24. S.G. Biedron, R.J. Dejus, W.J. Berg, P.K. Den Hartog, M. Erdmann, H.P. Freund, E. Gluskin, Z. Huang, K.-J. Kim, J.W. Lewellen, Y. Li, A.H. Lumpkin, S.V. Milton, E.R. Moog, A. Nassiri, V. Sajaev, G. Wiemerslage, and B.X. Yang, "Measurements of Nonlinear Harmonic Generation at the Advanced Photon Source's SASE FEL," Nucl. Instrum. Meth. A, accepted and in press.
25. V. Sajaev, W.J. Berg, S.G. Biedron, R.J. Dejus, P.K. Den Hartog, M. Erdmann, Z. Huang, K.-J. Kim, J.W. Lewellen, Y. Li, A.H. Lumpkin, O. Makarov, S.V. Milton, E.R. Moog, and E.M. Trakhtenberg, "Z-dependent Spectral Measurements of SASE FEL at APS," Nucl. Instrum. Meth. A, accepted and in press.
26. A.H. Lumpkin, W.J. Berg, S.G. Biedron, M.D. Borland, R.J. Dejus, M. Erdmann, J.W. Lewellen, Y. Li, S.V. Milton, E.R. Moog, V. Sajaev, B.X. Yang, "First Observations of Electron-Beam Microbunching in the Ultraviolet at 265 nm Using COTR in a SASE FEL," Nucl. Instrum. Meth. A, accepted and in press.
27. J.W. Lewellen et al., "Present Status and Recent Results from the APS SASE FEL," Nucl. Instrum. Meth. A, accepted and in press.
28. G. Isoyama et al., "Wavelength Spectra of Self-Amplified Spontaneous Emission in the Far-Infrared Region," Proc. of the 22nd International Free-Electron Laser Conference and 7th FEL Users Workshop, 13 to 18 August 2000, Durham, North Carolina, USA, to be published.
29. R. Kato et al., "Higher Harmonic Generation Accompanied by SASE in the Far-Infrared Region," submitted to Nucl. Instrum. Meth A.
30. A. Tremaine et al., "Experimental Characterization of SASE FEL Harmonic Radiation at Saturation," submitted to Nucl. Instrum. Meth A.
31. W.M. Fawley, "An Informal Manual for GINGER and its post-processor XPLOTGIN," LBNL-49625, 2002.
32. N.M. Kroll, P.L. Morton, and M.R. Rosenbluth, IEEE J. Quant. Electron. QE-17 (1981) 1436.
33. H.P. Freund and T.M. Antonsen, Jr., Principles of Free-electron Lasers (Chapman & Hall, London, 1986), 2nd edition.
34. H.P. Freund, Phys. Rev. E 52 (1995) 5401.
35. S.G. Biedron, H.P. Freund, and S.V. Milton, "Development of a 3D FEL code for the simulation of a high-gain harmonic generation experiment," in Free Electron Laser Challenges II, Harold E. Bennett, David. H. Dowell, eds., Proceedings of SPIE, 3614 (1999) 96.
36. G. Dattoli, M. Galli, and P.L. Ottaviani, "1-Dimensional Simulation of FEL Including High Gain Regime Saturation, Prebunching, and Harmonic Generation," ENEA internal report RT/INN/93/09 (1993).
37. D. Prosnitz, A. Szole, and V.K. Neil, Phys. Rev. A 24 (1981) 1436.
38. E.T. Scharlemann, J. Appl. Phys. 58 (1985) 2154.
39. S. V. Milton et al., originally published in Science Express as 10.1126/science.1059955 on May 17, 2001 and Science 292 (2001) 2037-2041 and references therein.
40. S. G. Biedron, H.P. Freund, S.V. Milton, L.-.H. Yu, and X.J. Wang, Nucl Instrum Meth A 475 (2001) 118.
41. D. Iracane, D. Touati, and P. Chaix, Nucl. Instrum. Meth. A 341 (1994) 230.
42. Asakawa et al., Nucl. Instrum. Meth. A 375 (1996) 416.
43. G. Dattoli, L. Gianessi, P.L. Ottaviani, H.P. Freund, S.G. Biedron, and S.V. Milton, "Two Harmonic Undulators and Harmonic Generation in High-Gain Free-Electron Lasers," submitted to Phys. Rev. E.
44. F. Ciocci, G. Dattoli, L. Giannessi, P. L. Ottaviani and A. Renieri, "Biharmonic Undulators and FEL Dynamics," Proc. of the 23rd International Free-Electron Laser Conference and 8th FEL Users Workshop, 20 - 24 August 2001, Darmstadt, Germany, to be published.